
Article:
Feng, Y., Renshaw, S. orcid.org/0000-0003-1790-1641 and Martin, P. (2012) Live imaging of tumor initiation in zebrafish larvae reveals a trophic role for leukocyte-derived PGE(2). Current Biology, 22 (13). pp. 1253-1259. ISSN 0960-9822

https://doi.org/10.1016/j.cub.2012.05.010

Current Biology 22, 1253–1259, July 10, 2012 ©2012 Elsevier Ltd. Open access under CC BY license. DOI 10.1016/j.cub.2012.05.010

Report

Live Imaging of Tumor Initiation in Zebrafish Larvae Reveals a Trophic Role for Leukocyte-Derived PGE_2

Yi Feng,[1,2,*] Stephen Renshaw,[3] and Paul Martin[1,*]
[1]School of Biochemistry and School of Physiology & Pharmacology, Biomedical Sciences Building, University of Bristol, University Walk, Bristol BS8 1TD, UK
[2]MRC Centre for inflammation Research, 47 Little France Crescent, Edinburgh, EH16 4TJ. UK
[3]MRC Centre for Developmental and Biomedical Genetics, The University of Sheffield, Firth Court, Western Bank, Sheffield, S10 2TN, UK

Summary

Epidemiology studies and clinical trials have suggested that the use of non-steroidal anti-inflammatory drugs (NSAIDs), including aspirin, can significantly reduce the incidence of and mortality associated with many cancers [1–3], and upregulation of the COX2-PGE_2 pathway in tumor microenvironments might drive several aspects of cancer progression [4–6]. For these reasons, the mechanisms linking COX blockade and cancer prevention have long been an area of active investigation [7]. During carcinogenesis, COX-2 is expressed both by malignant epithelial cells [8, 9] and by tumor-associated stromal cells, including macrophages [10–12], but the observation that NSAIDs are most effective in cancer prevention in $APC^{min/+}$ mice if the mice are treated from conception [13] suggests that the COX-2/PGE_2 pathway might also be critical at the earliest stages of tumor development. In this study we take advantage of the translucency and genetic tractability of zebrafish larvae to investigate the involvement of inflammatory cells at cancer initiation, when transformed cells first arise in tissues. We previously showed that innate immune cells supply early transformed cells with proliferative cues [14] and, by using complementary pharmacological and genetic experiments, we now show that prostaglandin E_2 (PGE_2) is the trophic signal required for this expansion of transformed cells. Our in vivo observations at these early stages of cancer initiation provide a potential mechanistic explanation for why long-term use of low doses of NSAIDs, including aspirin, might reduce cancer onset.

Results and Discussion

We have used a human $HRAS^{G12V}$-driven transgenic zebrafish cancer model, in which mucous-secreting cells (analogous to human goblet cells) in the skin are transformed by an eGFP-$HRAS^{G12V}$ fusion protein. Using this model, we have previously shown with a live imaging approach that $HRAS^{G12V}$ (hereafter referred to as V12RAS)-expressing transformed cells induce a robust inflammatory response immediately after their emergence in host skin [14]. Paradoxically, the recruited innate immune cells play a trophic role in promoting the growth of transformed cells [14]. To test whether the COX-2/PGE_2 pathway might be involved in this process, we decided to block PGE_2 production.

Blocking PGE_2 Synthesis Retards the Growth of Transformed Cells

PGE_2 is one of the most abundant PGs produced in the body and plays key roles in mediating the inflammatory response [7, 15]. Cyclooxygenase 1 and 2 (COX-1 and COX-2) catalyze the rate-limiting step in PGE_2 synthesis by converting arachidonic acid into prostaglandin H_2, which is subsequently converted to prostaglandins (PGs) via the actions of specific PG synthases (Figure 1A). COX-1 is the housekeeping enzyme that generates PGE_2 under normal conditions. COX-2 is induced under inflammatory conditions and generates PGE_2 via mPGES at the site of immune cell recruitment (Figure 1A).

Zebrafish have three COX enzymes, zfCOX-1, zfCOX-2a, and zfCOX2-b [16, 17], and two PGE_2 synthases, cytosolic PGE_2 synthase (cPGES) and microsomal PGE_2 synthase (mPGES) [18]. Because zebrafish larvae are amenable to chemical treatment, we first took a pharmacological approach to suppress PGE_2 production (as outlined in Figure 1B). Suppression of COX-2 by either NS398 or Celecoxib led to a significant reduction in the number of $V12RAS^+$ cells (Figure 1C; Figure S1 in the Supplemental Information available online) without altering expression levels of endogenous *kit a* (the transgene driver) or having adverse effects on larval development (Figure S1). Moreover, ectopically added $dmPGE_2$ (a stable analog of PGE_2) partially restored the number of transformed cells in COX-2-inhibitor-treated larvae (Figures 1D and 1E; Figure S1). No significant reduction in the number of $V12RAS^+$ cells was seen in larvae treated with the COX-1 inhibitor SC560 (Figure 1C). These data suggest that in zebrafish, COX-2-mediated production of PGE_2 promotes the growth of transformed cells.

To establish whether PGE_2 was indeed the main tumor-promoting mediator generated by COX-2 in our model, we used CAY10560, another inhibitor specific to mPGES, which is known to be downstream of COX-2 in generating PGE_2 in zebrafish [18]. Again, we saw a reduction in the number of transformed cells; $dmPGE_2$ was able to restore the number of transformed cells in combined treatment with CAY10560 (Figure 1F).

Both $V12RAS^+$-Transformed Cells and Recruited Leukocytes Express COX-2, but Only Leukocytes Express mPGES

In mammals, both cancer cells and stromal cells can upregulate COX-2 [8–11], although the contribution of immune-cell-derived PGE_2 in tumor progression has not yet been defined [5]. We wanted to identify which cell lineages expressed PGE_2-generating enzymes at the earliest tumor-initiation stage. Double immunostaining showed that both $V12RAS^+$ cells (transformed cells) and most L-plastin$^+$ cells (neutrophils and macrophages) expressed COX-2 (Figures 1H and 1I). However, we could only detect a signal for mPGES antibody in a subset (approximately 20%) of the recruited leukocytes and in none of the transformed cells (Figures 1J and 1K). These expression profiles imply that, at this early stage, only leukocytes generate PGE_2.

*Correspondence: v1yfeng2@staffmail.ed.ac.uk (Y.F.), paul.martin@bristol.ac.uk (P.M.)

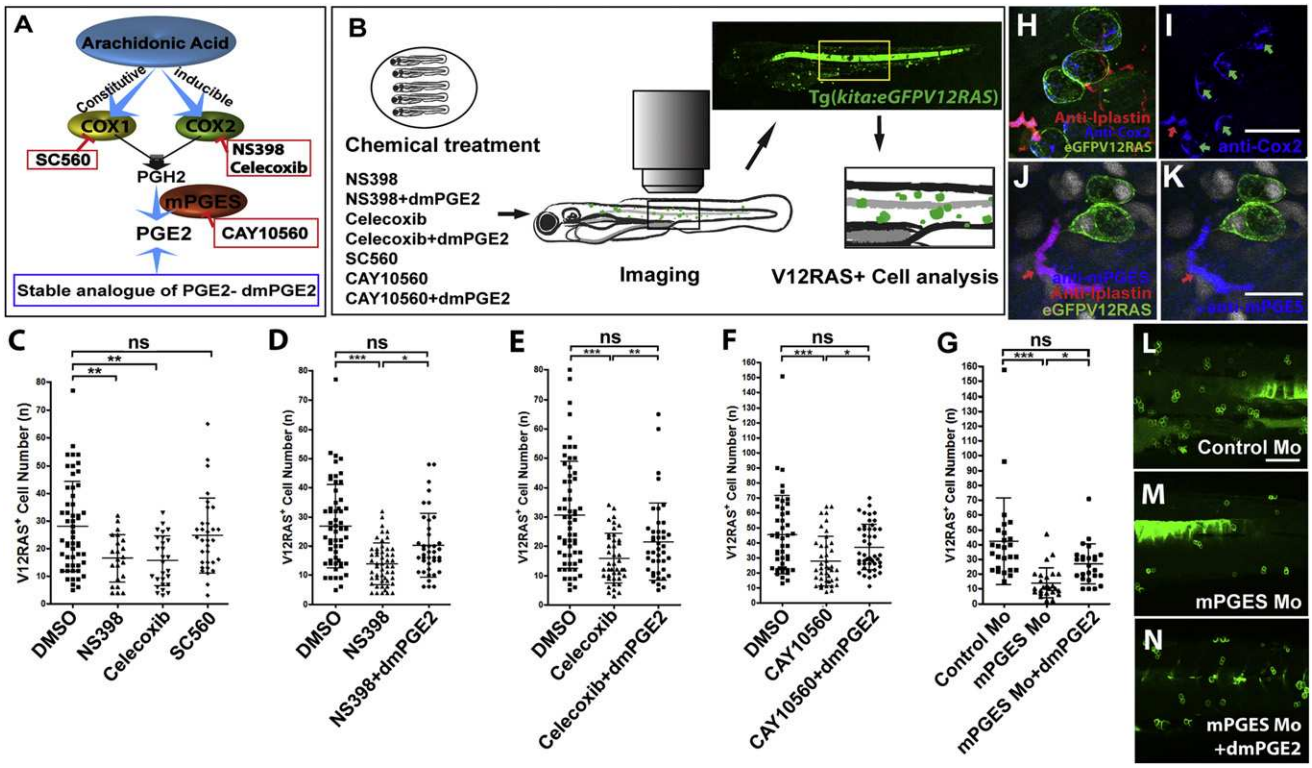

Figure 1. Blocking COX-2-mPGES-Mediated PGE_2 Production Suppresses the Growth of $V12RAS^+$ Transformed Cells In Vivo

(A) A schematic representation of PGE_2 production through the COX-2 pathway indicates the targets and inhibitors used in this study.

(B) A schematic representation of our pharmacological treatment regime and clonal analysis of transformed cells (green) in $V12RAS^+$-cell-bearing larvae. A yellow box indicates the flank skin region in which we quantified alterations in growth of $V12RAS^+$ cells.

(C–G) Graphic comparisons of $V12RAS^+$ cell numbers in larval flank skin region after various treatments; (C) larvae treated with DMSO, COX-1 inhibitor, SC-560, and the COX-2 inhibitors NS398 and Celecoxib ($p < 0.01$, n = 22, 27, and 32, respectively); (D) larvae treated with DMSO, NS398, and NS398 +dmPGE2 ($p < 0.001$, n = 56, 51, and 40, respectively); (E) larvae treated with DMSO, Celecoxib, and Celecoxib +dmPGE2 ($p < 0.001$, n = 61, 42, and 42, respectively); (F) larvae treated with DMSO, CAY10560 and CAY10560 +dmPGE2 ($p < 0.001$, n = 45, 42, and 46, respectively); (G) Control morphants, mPGES morphants, and mPGES morphants rescued with $dmPGE_2$ ($p < 0.001$, n = 26, 25, and 25, respectively).

(H) Immunostaining for COX-2 (blue) indicates that both leukocytes (anti-L-plastin [red]) and $V12RASeGFP^+$ transformed cells (green) express COX-2.

(I) Single-channel image of (H), better showing COX-2 expression; green and red arrows indicate transformed cells and leukocytes, respectively.

(J) Immunostaining for mPGES (blue) indicates its expression by some leukocytes (anti-L-plastin; red arrow) but not transformed cells (green).

(K) Single-channel image of (J).

(L–N) Representative images of flank skin regions showing $V12RAS^+$ clones (green) of (L) control morphant, (M) mPGES morphant, and (N) mPGES morphant supplemented with $dmPGE_2$- Scale bars represent 20 μm (H and I), 15 μm (J and K), and 100 μm (L–N). See also Figures S1, S2, and S3.

Morpholino Knockdown of mPGES Expression Confirms that PGE_2 Is Required for $V12RAS^+$ Overgrowth

Our inhibitor data had demonstrated that COX-2-mPGES-derived PGE_2 was important for $V12RAS^+$ cell growth. To confirm these findings, we used antisense morpholinos to genetically knock down PGE_2 production. Zebrafish have two genes encoding COX-2 but only one encoding mPGES. Moreover, mPGES only catalyzes PGE_2 production, and so we used a previously published mPGES morpholino to block its expression [19] (Figure S2). Unfortunately, mPGES-mediated PGE_2 is required for cell movements during epiboly [19]. To bypass this problem, we rescued normal early development of mPGES morphants by incubating them in $dmPGE_2$.Then, after epiboly, we transferred half of the morphants into fresh medium without $dmPGE_2$ at 48 hr post-fertilization (hpf; Figure S3); $V12RAS^+$ cell numbers were analyzed at 4.5 days post-fertilization (dpf). Again, we saw a reduction in the number of $V12RAS^+$ cells in mPGES morphants compared with control-morpholino-injected larvae (Figures 1G, 1L, and 1M), but the number of $V12RAS^+$ cells was partially restored in those mPGES morphants that continued with $dmPGE_2$ treatment (Figures 1G, 1L, and 1N).

In summary, both our pharmacological inhibition and genetic mPGES knockdown data suggest that PGE_2 plays an important role in promoting the growth of $V12RAS^+$-transformed cells, and our immunostaining data suggest that recruitment of immune cells might be the main source of PGE_2 at this stage. However, because ectopic $dmPGE_2$ failed to completely restore the growth of transformed cells to control levels in either our pharmacological-inhibition or genetic-knockdown experiments, it seems likely that there are also some PGE_2-independent influences on the growth of transformed cells.

PGE_2 Directly Promotes the Growth of Transformed Cells via the EP1 Receptor

To address whether PGE_2 exerts a direct effect on the growth of transformed cells, we next focused on which of the PGE_2 receptors was expressed by the transformed cells to mediate such a response. Our immunostaining data indicate that, of the

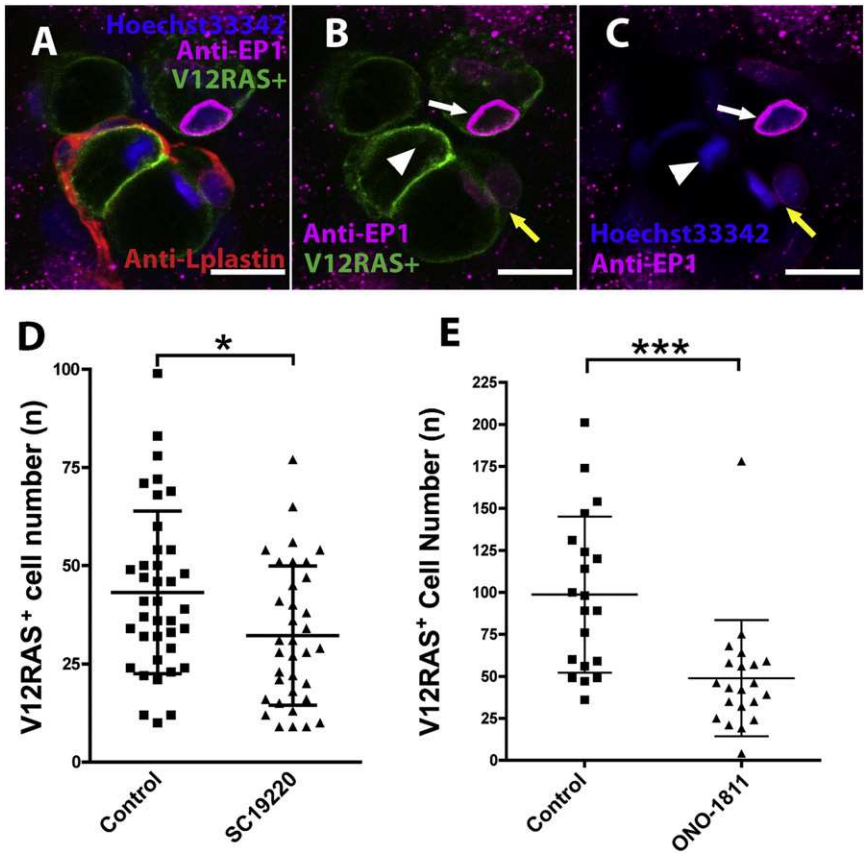

Figure 2. PGE_2 Promotes Growth of Transformed Cells via the EP1 Receptor

(A–C) Immunostaining for EP1 receptor showing EP1 (magenta) localized within V12RASeGFP$^+$ cells (green); nuclei are stained with Hoechst 33342 (blue), and leukocytes are revealed by immunostaining with anti-L-plastin antibody (red). EP1 receptor (magenta) shows perinuclear localization (white arrows in [B] and [C]); a pair of recently divided daughter transformed cells exhibit faint EP1 staining (yellow arrows in [B] and [C]), and a transformed cell at metaphase shows no EP1 signal (white arrowhead in [C]). Scale bars represent 10 μm.

(D) Graphic illustration showing that EP1 receptor antagonist SC19220 leads to a reduction in the number of transformed cells ($p < 0.05$, $n = 38$ and 35).

(E) The same is true for the EP1 receptor antagonist ONO-1811 ($p < 0{,}001$, $n = 20$ and 21).

See also Figure S1.

five PGE_2 receptors that exist in the zebrafish genome (ENSEMBL Zv9), only EP1 is highly expressed by the transformed cells (Figures 2A–2C) and has a particularly pronounced perinuclear localization, as previously reported for EP1 receptor localization in tissue cultured mammalian cells [20]. To test whether EP1 receptor was responsible for mediating the PGE_2 signal in transformed cells, we used two EP1-specific inhibitors, SC19220 and ONO-8711 (Cayman Chemicals), and both treatments led to a significant reduction in the growth of transformed cells in vivo (Figures 2D and 2E) without adverse effects on larval development (Figure S1). It is thus likely that PGE_2 promotes the growth of transformed cells through the EP1 receptor.

An Ectopic Supplement of $dmPGE_2$ Can Partially Restore V12RAS$^+$ Cell Growth in Leukocyte-Depleted Larvae

Our data herein suggest that PGE_2 is produced by leukocytes as trophic support for the growth of transformed cells. If this is indeed the case, then we should be able to restore tumor growth in leukocyte-depleted larvae by adding PGE_2. We thus blocked leukocyte development by using a combined morpholino *pu.1+gcsfr* double knockdown, which effectively arrests all myeloid lineage development in zebrafish larvae until at least 4 dpf [21]. Leukocyte depletion does not affect general embryo development (Figure S4A–S4G); however, this absence of leukocytes led to a dramatic reduction in the number of V12RAS$^+$ cells (Figures 3B and 3J). When we supplied $dmPGE_2$ to the leukocyte-depleted double morphants, we saw a partial restoration of V12RAS$^+$ cell numbers (Figures 3C and 3J). These data suggest that immune cell trophic support is mediated through the PGE_2-EP1 receptor pathway, which acts directly on the transformed cells.

$dmPGE_2$ Fully Restores V12RAS$^+$ Cell Numbers in Macrophage-Depleted Larvae but Only Partially Does So in Neutrophil-Deficient Larvae

In our previous studies, we found that the transformed cells trigger recruitment of several innate immune cell lineages [14]. We now wished to dissect the contribution of individual leukocyte lineages to the growth of transformed cells. In zebrafish, neutrophil development is severely impaired in *gcsfr*-morpholino-injected larvae, whereas macrophage numbers are only slightly decreased [21] (Figure S4K). In such neutrophil-depleted morphants, we observed that V12RAS$^+$ cell numbers are reduced almost to the numbers seen in *pu.1+gcsfr* morphants (which lack both neutrophils and macrophages; Figures 3B and 3D; Figure S4I). This suggests an important trophic role for neutrophils during the initial expansion of transformed cells.

IRF8 is a transcription factor that regulates the differentiation of a common progenitor into macrophages rather than neutrophils, and *irf8* morpholino treatment depletes macrophages and results in a compensatory increase in neutrophils [22] (see Figure S4J). In these macrophage-depleted larvae, we again saw a reduction in the number of V12RAS$^+$ cells (reduced to 41.9%) but to a much lesser degree than in total leukocyte (*pu1+gcsfr* morphant, macrophage + neutrophil)-depleted larvae (reduced to 21.1%) (Figures 3B, 3F, and 3J). We confirmed that macrophage depletion alone (i.e., without a compensatory increase in neutrophils) also leads to a reduction in the number of V12RAS$^+$ cells number (reduced to 49%) by using low-dose *pu.1* morpholino (Figures 3H and 3L). These data suggest that macrophages contribute to the trophic support of transformed cells but to a lesser extent than neutrophils.

Moreover, the nature of trophic support received from neutrophils could be qualitatively different from that received from macrophages. When $dmPGE_2$ was used to treat larvae

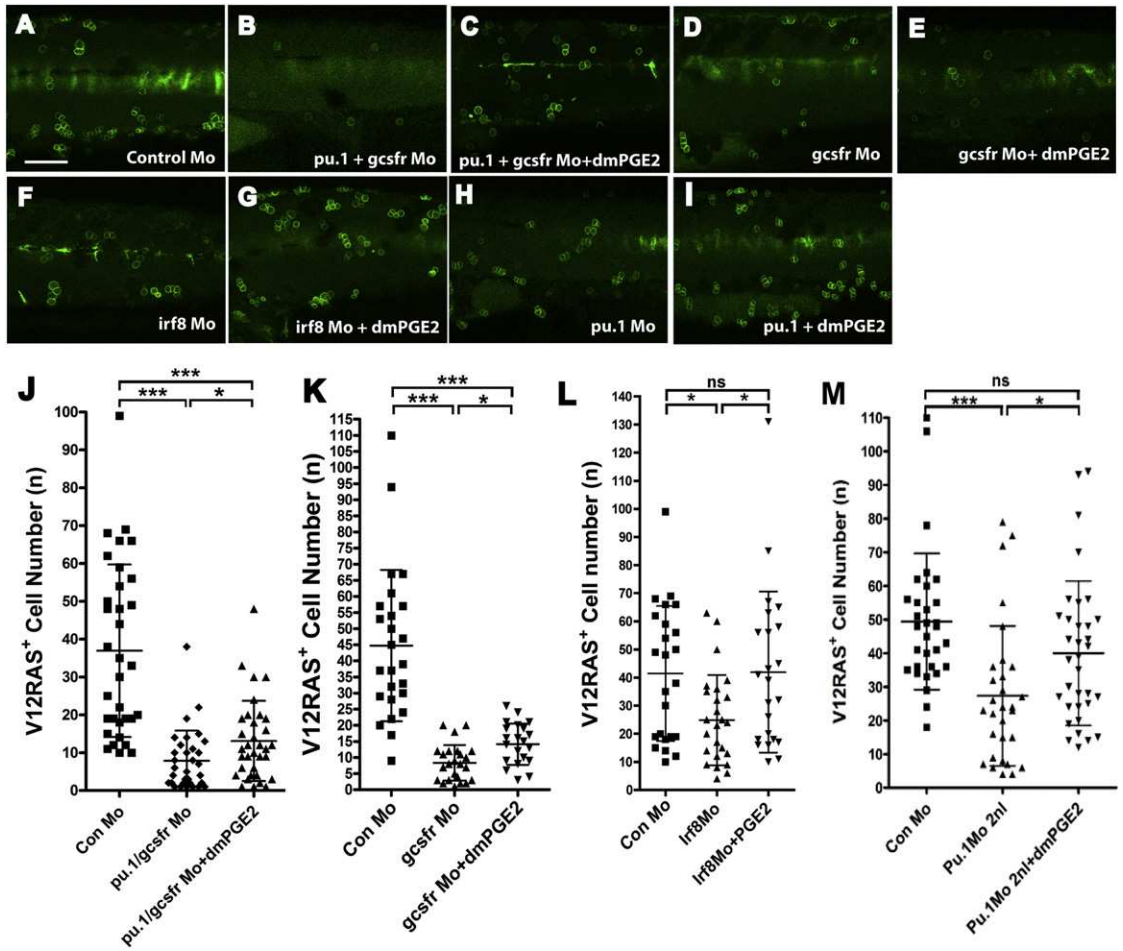

Figure 3. Leukocyte Depletion Prevents V12RAS$^+$ Cell Growth, which Can Be Partially Rescued by dmPGE$_2$

(A–I) Representative images of flank skin regions illustrating numbers of V12RASeGFP$^+$ transformed cells after morpholino (Mo) knockdown of *pu.1* and *gcsfr* (for depletion of both neutrophils and macrophages); *gcsfr* alone (for depletion of neutrophils); *irf8* or a lower dose (2 nl/embryo) of *pu.1* morpholino alone (for depletion of macrophages) with or without additional treatment with dmPGE$_2$.

(J) Graphic illustration of how dmPGE$_2$ can rescue the number of transformed cells in morphants in which both neutrophils and macrophages have been specifically depleted ($p < 0.01$, n = 33, 32, and 34).

(K) Graphic illustration of how dmPGE$_2$ can only partially rescue morpholino knockdowns that largely target neutrophils ($p < 0.001$, n = 25, 25, and 22).

(L and M) Similar graphic illustration of how dmPGE$_2$ can rescue morpholino knockdowns that largely target macrophages (irf8 Mo—$p < 0.05$, n = 24, 26, and 23; 2 nl pu.1 Mo—$p < 0.05$, n = 31, 30, and 34).

The scale bar represents 100 μm. See also Figures S3 and S4.

that had been depleted of different immune cell types, we saw differences in the rescue profile of transformed-cell growth. In both *pu.1+gcsfr* double morphants (lacking both macrophages and neutrophils) and *gcsfr* morphants (lacking only neutrophils), dmPGE$_2$ only partially restored V12RAS$^+$ cell numbers (Figures 3C, 3E, 3J, and 3K). However, in macrophage-depleted *irf8* morphants and low-dose *pu.1* morphants, dmPGE$_2$ treatment completely restored the number of transformed cells (Figures 3G, 3I, 3L, and 3M). It has previously been shown that PGE$_2$ can drive hematopoietic stem cell expansion [23], and so we tested whether leukocyte rescue by dmPGE$_2$ treatment might indirectly cause increased numbers of transformed cells, but we saw no significant recovery of depleted innate immune cells in these larvae (Figures S4I–S4N). These findings suggest that macrophages contribute PGE$_2$ alone, whereas neutrophils might produce other trophic factor(s).

Reduced PGE$_2$ Production Leads to Altered Neutrophil Migration in the Vicinity of Transformed Cells, and Increased Cell Death of Transformed Cells Follows along with Their Rapid Engulfment by Macrophages

It has been shown that PGE$_2$ regulates immune cell function, and several recent reports suggest that PGE$_2$ might induce an immunosuppressive phenotype in leukocytes [24–26]. We wondered whether suppressing PGE$_2$ production with COX-2 inhibitors might modulate the early inflammatory response and change the way in which leukocytes and transformed cells interact.

Cell-tracking analysis of time-lapse movies show that in COX-2 inhibitor (NS398)-treated larvae, neutrophils near clones of transformed cells show considerably reduced motility (migration velocity drops from 0.125 ± 0.046 μm to 0.054 ± 0.038 μm, [mean ± SD]) (Figures 4A, 4A′, 4B, 4B′, and 4C; also see Movie S1) in comparison to those in untreated

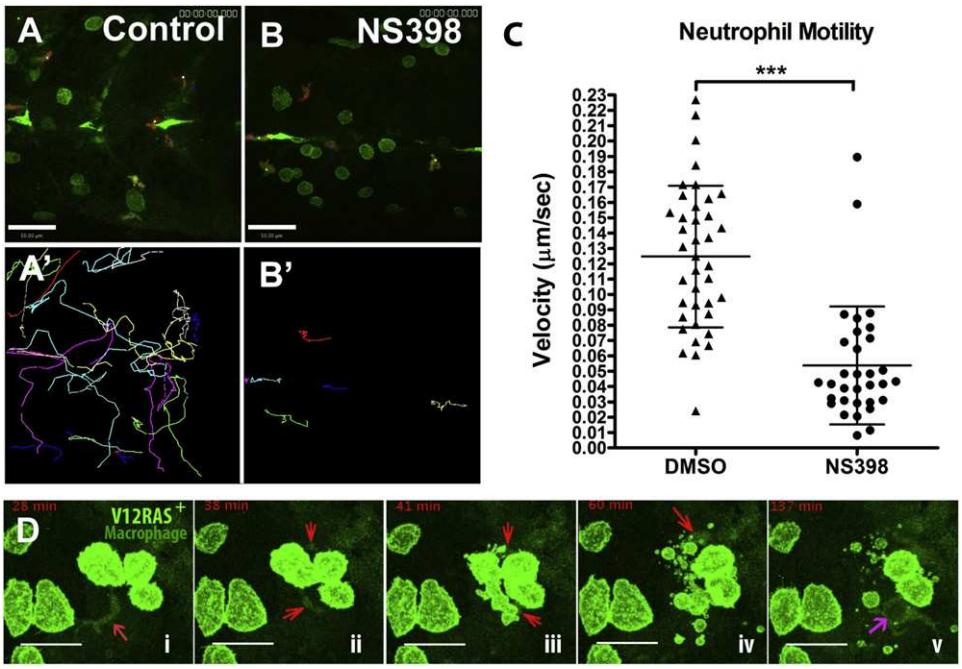

Figure 4. Live Imaging Reveals that Reduced PGE_2 Levels as a Result of COX-2 Inhibition Lead to Leukocyte Behavior Change and Increased Transformed-Cell Death

(A and B) Still images from movies illustrating neutrophil (red) numbers and their motility in the vicinity of V12RAS transformed cells (green) in (A) control and (B) NS398-treated larvae (images are taken from Movie S1) (A′ and B′) show the tracks over 100 min of neutrophil movements from the two movies S1A and S1B, respectively, revealing reduced neutrophil motility in NS398-treated (B′) compared with control (A′) larva. Scale bars represent 50 μm.

(C) Quantification of neutrophil migration velocity (V = mean ± SD); DMSO-treated V = 0.125 ± 0.046 μm (n = 39); NS398-treated V = 0.054 ± 0.038 μm (n = 32).

(D) A series of still images from a time-lapse movie (see Movie S2) showing transformed-cell death associated with a macrophage encounter in a larva treated with NS398; subsequently, this macrophage and others engulf the resulting cell debris. Red arrows in (i)–(iv) indicate a macrophage labeled by NFκB-RE:eGFP (pale green). Purple arrow in (v) indicates a macrophage engulfing the transformed-cell debris and forming a phagosome inside its cell body. The scale bar represents 15 μm.

transformed-cell-bearing larvae, indicating that reduced PGE_2 does indeed lead to a change in neutrophil behavior.

Live-imaging studies by us and others have defined the "inflammatory macrophage" in zebrafish larvae by their typical elongated, dendritic morphology and slow patrolling behavior [14, 27]. Here we used *Tg* (*NFκB-RE:eGFP; LysC:DsRed; kit a:GalTA4;UAS:eGFPV12RAS*) larvae, in which macrophages are labeled with low levels of NFκb reporter GFP (Figure 4D; also see Movie S2) to reveal their behavior near clones of transformed cells. In untreated larvae, transformed-cell deaths are sufficiently rare that we have never captured them by live imaging in either the presence or the absence of immune cells [14]. By contrast, in larvae treated with COX-2 inhibitor (NS398), we frequently saw transformed-cell deaths, and often these were associated with prior macrophage encounters (Figure 4D; see also Movie S2). The corpses of transformed cells were subsequently rapidly cleared away by adjacent macrophages. These data suggest that reduction of PGE_2 levels by COX-2 inhibition leads to a change of macrophage behavior and enhanced proinflammatory activity, which results in a more active engagement and engulfment of transformed cells. This is consistent with recent reports that PGE_2 directs macrophages toward a tumor-promoting M2 phenotype [24, 28] and can redirect dendritic cells toward a stable myeloid-derived-suppressor-cell phenotype [25].

Our previous and current studies reveal a pivotal contribution of host immune cells to the optimal growth of transformed cells as they first arise in tissues [14]. Here we show that leukocyte-derived PGE_2 is a key trophic factor for transformed cells at these early stages of cancer initiation. Our data suggest that PGE_2 might work in two complementary ways, both directly on transformed cells via the EP1 receptor and indirectly by promoting a "trophic inflammatory cell" behavior in neutrophils and macrophages; this behavior might also support the survival of transformed cells by inhibiting killing and engulfment.

We have provided evidence here that a trophic inflammatory response is important for a transformed cell to grow at its inception and that PGE_2 produced by innate immune cells via the COX-2 pathway is a key trophic factor for optimal growth of transformed cells at the earliest stages of tumor progression. Moreover, this trophic inflammatory response can be suppressed by the inhibition of PGE_2 production via COX-2 inhibitors, which might explain why use of non-steroidal anti-inflammatory drugs (NSAIDs) can reduce cancer incidence.

Experimental Procedures

Zebrafish Strains and Maintenance

Adult zebrafish (*Danio rerio*) were maintained as previously described [29]. All experiments were conducted with local ethical approval from the University of Bristol and in accordance with UK Home Office regulations. Strains included *Tg(5XUAS:eGFP-H-RASV12)io6* [30], *Et(kit a:GalTA4,UAS:mCherry)hzm1* [30], *Tg(LysC:DsRed)nz* [31]; the *Tg(NFκB-RE:eGFP)i235* line was generated with the method and constructs described in Kanther et al. [32].

Morpholino Injection

All morpholinos were obtained from (GeneTools LLC, Philomath, OR, USA) and injected into one-cell-stage embryos as previously described [19, 21, 22, 33]. For sequence information, see Supplemental Experimental Procedures.

Immunofluorescence, Live Imaging, and Tracking of Cell Movements in Larvae

Whole-mount immunostaining was performed as previously described [14]. For all our live-imaging studies, time-lapse movies were collected with a Leica SP5-AOBS Confocal Laser-Scanning Microscope. An Image J 1.4, Manual Tracking plugin was used for cell tracking (further details are available in the Supplemental Experimental Procedures).

Pharmacological Treatment and Clonal Analysis of the Progression of Transformed Cells

Transformed-cell-bearing larvae were treated with inhibitors of PGE_2-synthesis enzymes or $dmPGE_2$ from 48 hpf to 88 hpf or from 48 hpf to 96 hpf in 0.3% Danieau's solution containing 1% DMSO. All the inhibitors were from Cayman Chemicals. For detailed procedures, see Supplemental Experimental Procedures.

Statistics

All the data were analyzed (Prism 4.1, GraphPad Software, La Jolla, CA, USA) with an unpaired two-tailed Student's t test for comparisons between two groups with a one-way ANOVA and appropriate post-test adjustment for comparisons of multiple groups.

Supplemental Information

Supplemental Information includes four figures, two movies, and Supplemental Experimental Procedures and can be found with this article online at doi:10.1016/j.cub.2012.05.010.

Acknowledgments

We thank Chris Paraskeva and Helena Smartt for useful discussions during the preparation of our manuscript and Nikolay Ogryzko for generation of the *NFκB* line; this study was funded by a Wellcome Trust program grant to P.M.

Received: March 1, 2012
Revised: April 10, 2012
Accepted: May 2, 2012
Published online: May 31, 2012

References

1. Rothwell, P.M., Wilson, M., Elwin, C.E., Norrving, B., Algra, A., Warlow, C.P., and Meade, T.W. (2010). Long-term effect of aspirin on colorectal cancer incidence and mortality: 20-year follow-up of five randomised trials. Lancet *376*, 1741–1750.
2. Ruder, E.H., Laiyemo, A.O., Graubard, B.I., Hollenbeck, A.R., Schatzkin, A., and Cross, A.J. (2011). Non-steroidal anti-inflammatory drugs and colorectal cancer risk in a large, prospective cohort. Am. J. Gastroenterol. *106*, 1340–1350.
3. Liao, L.M., Vaughan, T.L., Corley, D.A., Cook, M.B., Casson, A.G., Kamangar, F., Abnet, C.C., Risch, H.A., Giffen, C., Freedman, N.D., et al. (2012). Nonsteroidal anti-inflammatory drug use reduces risk of adenocarcinomas of the esophagus and esophagogastric junction in a pooled analysis. Gastroenterology *142*, 442–452, e5, quiz e22–e23.
4. Mantovani, A., Allavena, P., Sica, A., and Balkwill, F. (2008). Cancer-related inflammation. Nature *454*, 436–444.
5. Greenhough, A., Smartt, H.J., Moore, A.E., Roberts, H.R., Williams, A.C., Paraskeva, C., and Kaidi, A. (2009). The COX-2/PGE2 pathway: key roles in the hallmarks of cancer and adaptation to the tumour microenvironment. Carcinogenesis *30*, 377–386.
6. Soumaoro, L.T., Uetake, H., Higuchi, T., Takagi, Y., Enomoto, M., and Sugihara, K. (2004). Cyclooxygenase-2 expression: A significant prognostic indicator for patients with colorectal cancer. Clin. Cancer Res. *10*, 8465–8471.
7. Wang, D., and Dubois, R.N. (2010). Eicosanoids and cancer. Nat. Rev. Cancer *10*, 181–193.
8. Glover, J.A., Hughes, C.M., Cantwell, M.M., and Murray, L.J. (2011). A systematic review to establish the frequency of cyclooxygenase-2 expression in normal breast epithelium, ductal carcinoma in situ, microinvasive carcinoma of the breast and invasive breast cancer. Br. J. Cancer *105*, 13–17.
9. Elder, D.J., Baker, J.A., Banu, N.A., Moorghen, M., and Paraskeva, C. (2002). Human colorectal adenomas demonstrate a size-dependent increase in epithelial cyclooxygenase-2 expression. J. Pathol. *198*, 428–434.
10. Hull, M.A., Booth, J.K., Tisbury, A., Scott, N., Bonifer, C., Markham, A.F., and Coletta, P.L. (1999). Cyclooxygenase 2 is up-regulated and localized to macrophages in the intestine of Min mice. Br. J. Cancer *79*, 1399–1405.
11. Bamba, H., Ota, S., Kato, A., Adachi, A., Itoyama, S., and Matsuzaki, F. (1999). High expression of cyclooxygenase-2 in macrophages of human colonic adenoma. Int. J. Cancer *83*, 470–475.
12. Williams, C.S., Tsujii, M., Reese, J., Dey, S.K., and DuBois, R.N. (2000). Host cyclooxygenase-2 modulates carcinoma growth. J. Clin. Invest. *105*, 1589–1594.
13. Sansom, O.J., Stark, L.A., Dunlop, M.G., and Clarke, A.R. (2001). Suppression of intestinal and mammary neoplasia by lifetime administration of aspirin in Apc(Min/+) and Apc(Min/+), Msh2(-/-) mice. Cancer Res. *61*, 7060–7064.
14. Feng, Y., Santoriello, C., Mione, M., Hurlstone, A., and Martin, P. (2010). Live imaging of innate immune cell sensing of transformed cells in zebrafish larvae: Parallels between tumor initiation and wound inflammation. PLoS Biol. *8*, e1000562.
15. Hata, A.N., and Breyer, R.M. (2004). Pharmacology and signaling of prostaglandin receptors: multiple roles in inflammation and immune modulation. Pharmacol. Ther. *103*, 147–166.
16. Grosser, T., Yusuff, S., Cheskis, E., Pack, M.A., and FitzGerald, G.A. (2002). Developmental expression of functional cyclooxygenases in zebrafish. Proc. Natl. Acad. Sci. USA *99*, 8418–8423.
17. Ishikawa, T.O., Griffin, K.J., Banerjee, U., and Herschman, H.R. (2007). The zebrafish genome contains two inducible, functional cyclooxygenase-2 genes. Biochem. Biophys. Res. Commun. *352*, 181–187.
18. Pini, B., Grosser, T., Lawson, J.A., Price, T.S., Pack, M.A., and FitzGerald, G.A. (2005). Prostaglandin E synthases in zebrafish. Arterioscler. Thromb. Vasc. Biol. *25*, 315–320.
19. Cha, Y.I., Kim, S.H., Sepich, D., Buchanan, F.G., Solnica-Krezel, L., and DuBois, R.N. (2006). Cyclooxygenase-1-derived PGE2 promotes cell motility via the G-protein-coupled EP4 receptor during vertebrate gastrulation. Genes Dev. *20*, 77–86.
20. Bhattacharya, M., Peri, K.G., Almazan, G., Ribeiro-da-Silva, A., Shichi, H., Durocher, Y., Abramovitz, M., Hou, X., Varma, D.R., and Chemtob, S. (1998). Nuclear localization of prostaglandin E2 receptors. Proc. Natl. Acad. Sci. USA *95*, 15792–15797.
21. Liongue, C., Hall, C.J., O'Connell, B.A., Crosier, P., and Ward, A.C. (2009). Zebrafish granulocyte colony-stimulating factor receptor signaling promotes myelopoiesis and myeloid cell migration. Blood *113*, 2535–2546.
22. Li, L., Jin, H., Xu, J., Shi, Y., and Wen, Z. (2011). Irf8 regulates macrophage versus neutrophil fate during zebrafish primitive myelopoiesis. Blood *117*, 1359–1369.
23. Durand, E.M., and Zon, L.I. (2010). Newly emerging roles for prostaglandin E2 regulation of hematopoiesis and hematopoietic stem cell engraftment. Curr. Opin. Hematol. *17*, 308–312.
24. Heusinkveld, M., de Vos van Steenwijk, P.J., Goedemans, R., Ramwadhdoebe, T.H., Gorter, A., Welters, M.J., van Hall, T., and van der Burg, S.H. (2011). M2 macrophages induced by prostaglandin E2 and IL-6 from cervical carcinoma are switched to activated M1 macrophages by CD4+ Th1 cells. J. Immunol. *187*, 1157–1165.
25. Obermajer, N., Muthuswamy, R., Lesnock, J., Edwards, R.P., and Kalinski, P. (2011). Positive feedback between PGE2 and COX2 redirects the differentiation of human dendritic cells toward stable myeloid-derived suppressor cells. Blood *118*, 5498–5505.
26. Kalinski, P. (2012). Regulation of immune responses by prostaglandin E2. J. Immunol. *188*, 21–28.
27. Mathias, J.R., Dodd, M.E., Walters, K.B., Yoo, S.K., Ranheim, E.A., and Huttenlocher, A. (2009). Characterization of zebrafish larval inflammatory macrophages. Dev. Comp. Immunol. *33*, 1212–1217.
28. Nakanishi, Y., Nakatsuji, M., Seno, H., Ishizu, S., Akitake-Kawano, R., Kanda, K., Ueo, T., Komekado, H., Kawada, M., Minami, M., and Chiba, T. (2011). COX-2 inhibition alters the phenotype of tumor-associated macrophages from M2 to M1 in ApcMin/+ mouse polyps. Carcinogenesis *32*, 1333–1339.

29. Westerfield, M. (2000). The zebrafish book. A guide for the laboratory use of zebrafish (Danio rerio), 4th ed (Eugene, OR: The University of Oregon Press).
30. Santoriello, C., Gennaro, E., Anelli, V., Distel, M., Kelly, A., Köster, R.W., Hurlstone, A., and Mione, M. (2010). Kita driven expression of oncogenic HRAS leads to early onset and highly penetrant melanoma in zebrafish. PLoS ONE *5*, e15170.
31. Hall, C., Flores, M.V., Storm, T., Crosier, K., and Crosier, P. (2007). The zebrafish lysozyme C promoter drives myeloid-specific expression in transgenic fish. BMC Dev. Biol. *7*, 42.
32. Kanther, M., Sun, X., Mühlbauer, M., Mackey, L.C., Flynn, E.J., 3rd, Bagnat, M., Jobin, C., and Rawls, J.F. (2011). Microbial colonization induces dynamic temporal and spatial patterns of NF-κB activation in the zebrafish digestive tract. Gastroenterology *141*, 197–207.
33. Rhodes, J., Hagen, A., Hsu, K., Deng, M., Liu, T.X., Look, A.T., and Kanki, J.P. (2005). Interplay of pu.1 and gata1 determines myelo-erythroid progenitor cell fate in zebrafish. Dev. Cell *8*, 97–108.